Highly Emissive Nanostructured Thin Films of Organic Host–Guests for Energy Conversion

Juliette Moreau,[b] Umberto Giovanella,[a] Jean-Philippe Bombenger,[a] William Porzio,[a] Varun Vohra,[a] Laura Spadacini,[b] Giuseppe Di Silvestro,[b] Luisa Barba,[c] Gianmichele Arrighetti,[c] Silvia Destri,[a] Mariacecilia Pasini,[a] Michele Saba,[d] Francesco Quochi,[d] Andrea Mura,[d] Giovanni Bongiovanni,[d] Mauro Fiorini,[e] Michela Uslenghi,[e] and Chiara Botta*[a]

All-organic nanostructured host–guest systems, based on dyes inserted in the nanochannels of perhydrotriphenylene (PHTP) and deoxycholic acid (DCA), show enhanced fluorescence properties with quantum yields even higher than those of the dyes in solution, thanks to the high concentration of emissive molecules with controlled spatial and geometrical organization that prevents aggregation quenching. Both host molecules crystallize, growing with the long axis oriented along the direction of the nanochannels where the line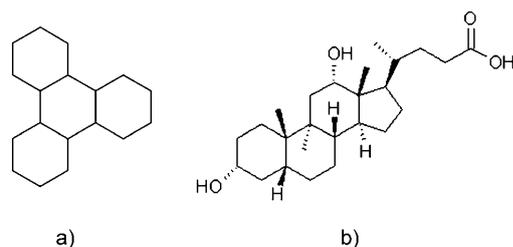ar-chain dyes are inserted, to yield crystals emitting well-polarized light. For the DCA-based host–guests, homogeneous thin films suitable for several applications are obtained. Colour emission in such films can be tuned by co-inclusion of two or three dyes due to resonant energy-transfer processes. We show that films obtained by low-cost techniques, such as solution casting and spin-coating, convert UV light into visible light with an efficiency much higher than that of the standard polymeric blends.

Introduction

The control of intermolecular interactions[1] is crucial to the exploitation of molecular semiconductors for organic electronics, and the incorporation of active molecules (light emitters, nonlinear optics, etc.) into a proper host matrix enables control of the spatial organization of the molecular assemblies. In particular, the incorporation of conjugated molecules possessing a "long" molecular axis in host compounds, such as urea, thiourea, tris-o-thymotide, perhydrotriphenylene (PHTP), deoxycholic acid (DCA), and cyclodextrins, yields channel-type inclusion compounds (ICs).[2] ICs provide materials with very high concentrations of active molecules possessing peculiar spatial and geometrical organizations that can be exploited for many applications. Another interesting aspect of the ICs is that they provide the opportunity to explore the photophysics of isolated, often oriented, molecules.[3–6]

A large study about the fabrication process, structure, and thermodynamic and optical properties of ICs, in which the guests consist of suitable conjugated molecules and the host is PHTP, has already been reported in the literature.[3,7] The

PHTP molecules (see Scheme 1) form stacks that give rise to hexagonally shaped channels with a typical inter-channel distance of 1.4 nm. PHTP ICs have been generally prepared by melting and successively cooling the powders,[3,4] by slow

[a] Dr. U. Giovanella, Dr. J.-P. Bombenger, Dr. W. Porzio, V. Vohra, Dr. S. Destri, Dr. M. Pasini, Dr. C. Botta
Istituto per lo Studio delle Macromolecole, C.N.R.
Via Bassini 15, 20133 Milano (Italy)
and
Polo Scientifico Tecnologico, CNR
Via Fantoli 16, 20133 Milano (Italy)
Fax: (+ 39) 0270636400
E-mail: chiara.botta@ismac.cnr.it

[b] Dr. J. Moreau,+ Dr. L. Spadacini, Prof. G. Di Silvestro
Dipartimento di Chimica Organica e Industriale
Università di Milano
Via Venezian 21, 20133 Milano (Italy)

[c] Dr. L. Barba, Dr. G. Arrighetti
Istituto di Cristallografia, CNR
Elettra Synchrotron Area Science Park
SS 14 Km 163.5 34012 Basovizza, Trieste (Italy)

[d] Dr. M. Saba, Dr. F. Quochi, Prof. A. Mura, Prof. G. Bongiovanni
Dipartimento di Fisica, CGS and SLACS-CNR
Università di Cagliari
09042 Monserrato, CA (Italy)

[e] Dr. M. Fiorini, Dr. M. Uslenghi
Istituto Nazionale di Astrofisica, sez. IASF Milano
Via Bassini 15, 20133 Milano (Italy)

[+] Current address:
ICMR-UMR CNRS 6229, UFR Sciences Exactes et Naturelles
Moulin de la Housse, BP 1039, 51687 Reims cedex 2 (France)

Supporting information for this article is available on the WWW under http://dx.doi.org/10.1002/cphc.200800682.

Scheme 1. Structures of the PHTP (a) and DCA (b) molecules.

evaporation of the solvent[5,8] or by thermal co-evaporation of the PHTP host and the guest.[9,10]

DCA is part of the bile salts family. It is commercially available and one of the oldest hosts that is able to include a large range of organic compounds.[11] Bile acids are planar amphiphilic compounds with one hydrophobic side (without hydroxyl groups) and one hydrophilic side (containing hydroxyl groups; see Scheme 1), which form unique bilayer structures with alternating stacks of hydrophobic and hydrophilic layers. The bent molecular shape of DCA provides molecular channels, or one-dimensional molecular cavities, running through the hydrophobic layer. Many hydrophobic organic guests can be included in this type of host framework. Intermolecular hydrogen bonding between steroidal α faces (hydrophilic faces) plays a key role in the robustness of the bilayer structure of DCA.[12] Until now, DCA has mainly been used in the medical domain for the treatment of bile acid deficiency or some liver diseases, and in the optical domain since the inclusion of achiral molecules inside the chiral DCA space led to a measurable circular dichroism.[13] The recent report that co-adsorption of DCA enhances the performances of dye-sensitized solar cells by suppression of dye π–π stacking[14] demonstrates that DCA can also play an important role in the field of optoelectronics.

Host–guest systems are ideal candidates for optoelectronic applications thanks to their high absorption cross-section and emission efficiency. Through a proper choice of the dyes, their absorption–emission properties can be easily tuned and self-absorption processes avoided. We have shown that by inserting two or three dyes in the channels of the PHTP host, materials able to convert energy from the UV to the visible with efficiencies as high as 100% can be obtained[15] as a result of the highly efficient resonant energy-transfer processes that occur among the guest molecules,[4] whose spatial and geometrical organization is imposed by the host. These systems are therefore ideal materials for energy conversion to be used as colour-changing media for light-emitting diodes, as light harvesters for solar cells or sensitizers for UV detectors. The main drawback of host–guest systems based on the PHTP host is their lack of processability in the form of thin uniform films, which are necessary for most of these applications. Indeed, PHTP host–guest systems have been obtained so far in the form of crystals or polycrystalline powders.

Herein, we studied the morphological and fluorescence properties of films based on all-organic ICs obtained with different preparation methods in order to obtain uniform films. To this end, herein we focus our attention on the DCA host and obtain the crystal structure of its IC with a highly emissive dye. We analyse DCA ICs with terphenyl (P3) and some dyes emitting in the blue, namely, terthiophene (T3), diphenylbutadiene (DPB) and 1,6-diphenyl-1,3,5-hexatriene (DPH), and compare their properties with those of the well-studied PHTP-based ICs. Co-inclusion compounds (co-ICs) of two or three different dyes in DCA allow the colour emission to be tuned down to the whole visible range. We demonstrate that quite homogeneous thin films of DCA ICs can be deposited by using the simple, low-cost spin-coating technique and show that cast and spin-coated films based on P3, DPB and DPH in DCA

are efficient energy converters from the near-UV (NUV) to the blue.

Results and Discussion

DCA and PHTP Host–Guest Crystals

Films of PHTP ICs were grown by thermal co-evaporation in high vacuum of the host and guest molecules on cooled substrates. The films are formed by small crystals of host–guest molecules whose dimensions and orientation depend on the substrate and evaporation conditions. However, we could not obtain uniform thin films of PHTP ICs with this technique. Figures 1 a,b show fluorescence images of T3-PHTP ICs obtained by thermal deposition on Si wafers and quartz plates. Small crystals are preferentially lying on the untreated quartz plate,
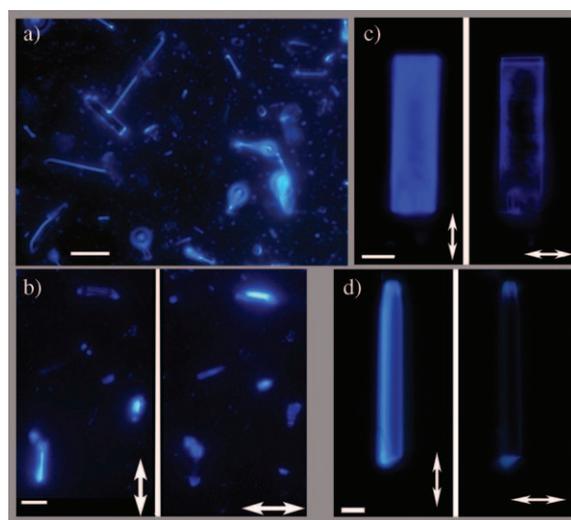

Figure 1. Polarized fluorescence microscopy images of T3-PHTP co-evaporated in high vacuum on a Si wafer (a) and a quartz plate (b). Crystals of DPB-DCA (c) and DPH-DCA (d) obtained from slow evaporation of methanol/ethyl acetate (2:4) solution. The arrows show the direction of the analyser axis. Scale bar: 5 μm.

while slightly bigger crystals are lying and standing on the Si wafer substrate. The bright fluorescent edges of the crystals grown on Si indicate the presence of out-coupling light[16] wave-guided inside the PHTP host. Polarized fluorescence images show that the co-evaporated crystals emit polarized light, similarly to crystals obtained from solution.[5]

Figures 1 c,d show fluorescence microscopy images of crystals of DCA ICs containing blue-emitting dyes, obtained from the slow evaporation of the solutions. DCA host–guest crystals show well-polarized light emission. This result demonstrates that the orientation of the dyes inserted in DCA is along the crystal axis, and therefore, that the DCA molecules crystallize growing with the long axis oriented along the direction of the nanochannels.

We studied in detail the crystal structure of the DPH-DCA IC, as reported in Figure 2, in comparison with the model structure of the PHTP IC. Similarly to PHTP, DCA ICs form crystals
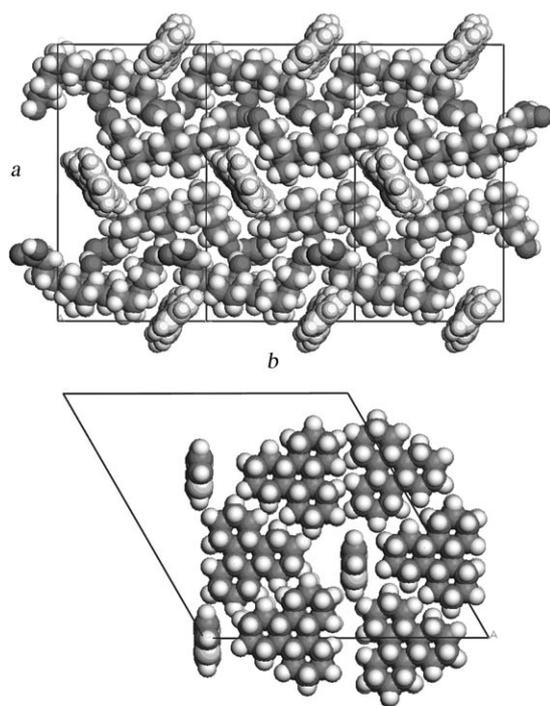
Figure 2. Crystal structure of a DPH-DCA IC crystal (top) and model structure of a T3-PHTP IC crystal (bottom), both viewed along the short *c* axis.

with parallel channels of about 1.4 nm separation where the linear-chain molecules are inserted. The DCA IC forms an orthorhombic crystal consisting of the packing of discrete DCA molecules, through the H-bond formation of adjacent carboxylic groups,[17] thus leaving two cavities in the unit cell where the guest molecule can be accommodated (see Figure 2, top). The channel developing along the *c* axis recalls a bowel shape; however, normal to the *ab* plane it seems approximately a parallelogram (minimum and maximum diagonals of 0.75 and 0.98 nm, respectively). The hole dimensions, after subtraction of van der Waals (vdW) radii, do not exceed 0.66×0.5 nm, hence allowing for the insertion of selected molecules, such as DPH. As regards the guest dimensions, the lengths of both DPH and the *c* axis can be compared to investigate the replenishment level of the guest molecule in the crystal. Differently from the oligothiophene case in PHTP,[18] no simple integer ratio between such lengths is observed (i.e. no commensurability) whatever conformation is adopted by the molecule, which indicates possible positional disorder along the channel. Namely, for the *trans–trans* case, the smaller integer ratio is five molecules distributed along with 12 unit cells. In spite of the presence of two different positions, that is, spatial disorder, a detailed refinement ($R = 0.07$) allows assessment of the complete channel replenishment (see the Supporting Information).

The examination of other guests in the same crystals is interesting—at least at the modelling level—in view of understanding the optical properties of host–guest complexes. The T3 molecule can be conveniently inserted into the channel with no stress for vdW interactions, as the overall length (1.041 nm) plus vdW contacts (1.40 nm) is smaller than double the *c* axis (1.45 nm). The DPB molecule is larger than the double unit cell

in both the conformations, that is, s-*trans* (1.165 nm) and s-*cis* (1.145 nm) plus vdW contacts; hence, to be inserted into the channel with acceptable stress, its axis should not be parallel to the *c* axis. Molecular model calculations[19] indicate an angle larger than 25°.

DCA Host–Guest Thin Films

Differently from the PHTP ICs, for which only crystals or polycrystalline powders and films can be obtained by using different preparation techniques, in the case of DCA we are also able to prepare thin films. Figure 3 shows fluorescence microscopy images of films obtained from DCA solutions of T3, DPB and DPH. Films prepared by solution casting (see Figures 3 a, c, e) display small-sized crystals that form inhomogeneous polycrystalline films. In the case of spin-coated films (Figures 3 b, d, f), we obtained more homogeneous films covering the whole substrate, which might be suitable as coatings for several applications. On the other hand, their morphology is far from planar (see the AFM height images in the inserts), displaying a roughness that depends on the solvent and the spinning rate. Indeed, the proper choice of surface roughness allows the control of waveguiding effects that reduce the total amount of light emitted from the surface.
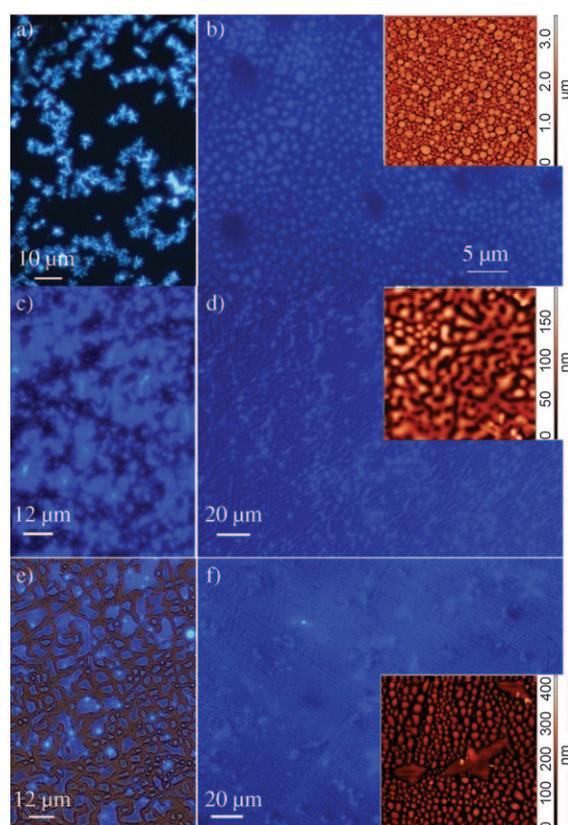

Figure 3. Fluorescence microscopy images of T3-DCA cast (a) and spin-coated (b) films. DPB-DCA cast (c) and spin-coated (d) films obtained from methanol solutions. Optical/fluorescence images of DPH-DCA cast (e) and spin-coated (f) films obtained from methanol/ethyl acetate. The insets in the images of the spin-coated films show the 20×20 μm AFM height images. Spin-coated films are obtained at 500 rpm.

Photoluminescence

The photoluminescence (PL) spectra of P3, T3, DPB and DPH are reported in Figure 4 for diluted solutions, aggregated molecules (obtained by solution casting) and the two ICs. No relevant changes are observed in the PL spectra of ICs prepared
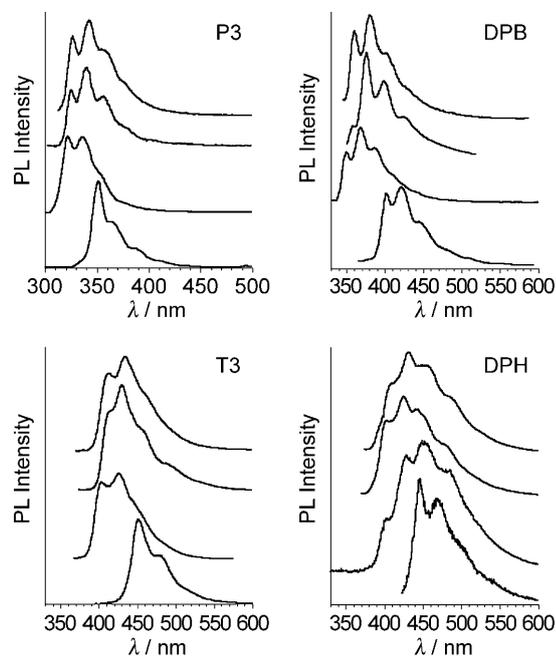

Figure 4. PL spectra of the molecules included in DCA and PHTP, dissolved in methanol and in the aggregate state (top to bottom). The spectra were recorded at room temperature and are displaced vertically for clarity. Films of DCA ICs were obtained by spin-coating from solution. P3, T3 and DPH in PHTP ICs were obtained by thermal co-evaporation; DPB in PHTP IC is obtained by powder melting.

with different techniques. Only a reduction of the intensity of the higher-energy component of the fluorescence is observed for crystals and thick films due to self-absorption effects.

The energy positions of the spectra of DCA ICs are slightly red-shifted with respect to the corresponding PHTP ICs. For all the molecules, the PL spectra of the ICs are very similar to those of the solutions while the emission of the aggregated molecules is red-shifted. The different absorption and PL properties of DPB *s*-*trans* and *s*-*cis* conformers have been used to study their equilibrium in solution[20] and photoisomerization processes in the solid state.[21] According to the preparation conditions of DPB and DPB-DCA, PL spectra of different mixtures of the two conformers are obtained (see the Supporting Information). Figure 4 shows spectra typical of the *trans* conformer. A photoisomerization process is observed for the DPB molecules in DCA similar to that observed for DPB crystals by Saltiel et al.,[21] even though we

found that its evolution is much slower than that observed for the DPB molecules cast from solution (see the Supporting Information). Moreover, while in DPB films a decrease of the overall PL intensity is detected after photoisomerization, in DCA ICs the emission intensity is stable after prolonged light-exposure times. DPB in PHTP IC does not show any photoisomerization process, which suggests that inclusion in the PHTP nanochannels, being slightly smaller than the DCA ones, prevents isomerization phenomena of the guest. DPH fluorescence of both the ICs shows spectral shapes resembling the emission from the 2^1A_g state of the all-*trans* DPH conformer.[22–25]

The main difference observed in the PL properties of the molecules possessing different aggregation states is the emission efficiency. As can be seen from the data reported in Table 1, the PL quantum efficiency (QY) of the dyes in the aggregate state is quite low due to aggregation quenching effects, whereas ICs show QYs comparable or even higher than in solution. The PL lifetimes of T3, DPB and DPH included in DCA are 0.2, 0.7 and 2.5 ns, respectively. These lifetimes are similar to those of the solutions and of the PHTP ICs (see Table 1). The presence of a fast initial decay for the DPB ICs may be related to a fast energy transfer from the *trans* to the *cis* conformers. The long lifetime of the DPH molecule is consistent with the forbidden nature of the transition from the lower excited energy state 2^1A_g and its value (as well as the QY) strongly depends on the polarizability of the environment,[10, 20, 26, 27] since the 1^1B_u energy position decreases more rapidly than the 2^1A_g one for increasing polarizability.[23, 24] The decay time of dyes in the aggregated state is faster and, in the case of DPH, is non-exponential due to aggregation quenching effects that give rise to a faster initial decay.[28]

To extend from the blue to the whole visible the range of the emission of DCA ICs, we inserted two or three dyes in the DCA host. Co-ICs of DPH and P3 in DCA show emission from the DPH chromophore when P3 is excited (see Figure 5), which indicates that in the DCA host crystal, similarly to the PHTP crystal,[4, 15] efficient resonant energy transfer shifts the emission far from the absorption region. The high PL QY (0.90) obtained for P3:DPH-DCA with 80:20 dye molar ratio shows that NUV light (absorbed by the P3 dye) is converted to the blue (emission of the DPH dye) without loss of energy. The addition of a small amount of the third dye quinquethiophene, or T5, emitting in the yellow–green region allows transfer of energy from the NUV to nearly the whole visible spectrum (see Figure 5) through a two-step resonant energy-transfer process.[15] The

Table 1. Optical properties of the ICs. PL QY and lifetimes.

Guest	Abs [nm]	Em [nm]	PL QY/lifetimes			
			DCA IC	PHTP IC	Solution	Film
T3	320–410	410–480	0.13/200 ps	0.09[10]/200 ps	0.07/170 ps	0.02/83 ps
P3	250–320	320–360	0.92	0.73[10]	0.82[10]	0.63[10]
DPB	280–350	350–450	0.46/0.12,0.7 ns	0.37/0.18,0.7 ns	0.42/0.6 ns[a, 26]	0.12
DPH	320–390	400–500	0.85/2.5 ns	0.65[15]/4 ns[15]	0.65/13 ns[a, 26]	0.03/ < 0.5 ns

[a] Different values are reported for different solvents.[10, 20, 26, 27]
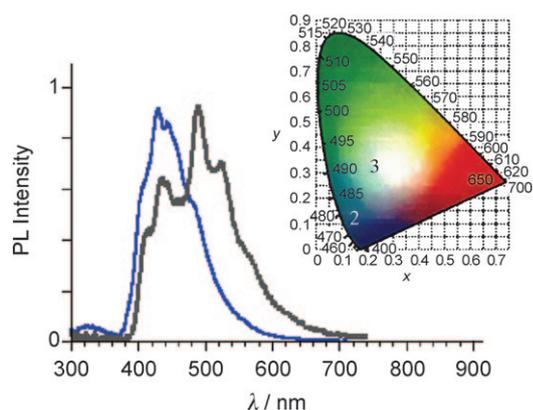
Figure 5. PL of P3:DPH-DCA (80:20; blue line) and P3:DPH:T5-DCA (50:48:2; grey line) cast films excited at 280 nm. Inset: CIE coordinates (0.14;0.11) for the two-dye IC and (0.22;0.31) for the three-dye IC.

Figure 6. a) Light intensity detected through DPB-DCA (bold line) and blends of DPB in PMMA (solid line), spin-coated (dashed line) and cast (thin line), with quartz substrate as reference (grey line). In the inset, the ratio *R* between the light detected with and without the sample in front of the detector head is reported for cast (solid line) and spin-coated (500 rpm, dotted lines; 1000 rpm, dashed–dotted line) films of DCA ICs for DPB (bold), DPH (thin) and P3:DPB (80:20) co-IC (grey).

emission therefore shifts from the blue (two-dye IC) to the nearly white emission region for the three-dye IC, as can be seen in the inset of Figure 5 where the CIE coordinates of the emissions are shown.

Energy Conversion

Silicon-based detectors, which largely rule the field of optical photosensors, suffer in the NUV region from a significant decrease in the QY. Therefore, for efficient NUV photon detection, the sensitivity of Si detectors is usually extended towards shorter wavelengths by coating the detector head with polymeric blends of organic dyes.[29] To measure the efficiency of energy conversion of DCA ICs from the NUV to the visible, we measured the light sensed by a standard Si detector, the sensitivity of which sharply decreases at wavelengths below 300 nm when a film of the material is placed in front of the detector head. We compared the light sensed when a film of DPB-DCA IC was placed in front of the detector head with that observed with a standard film of DPB blended in poly(methyl methacrylate) (PMMA), without any optimization of the optical coupling between the sample and the detector.

As shown in Figure 6, the IC increases the total amount of light sensed by the detector in the UV range with an efficiency of conversion much higher than that of the standard polymeric film. The better performances of the IC can be related both to the peculiar morphology of the films, which reduces the waveguiding losses present in planar polymeric films (spin-coated blend), and to the higher efficiency of emission of the dyes included in the DCA structure (PL QYs are about 2–2.5 times higher than those of PMMA blends).

In the inset of Figure 6 the ratio *R* between the light sensed with and without the sample is reported for different films of ICs and co-ICs. For both DPB and DPH dyes, we found that cast or spin-coated films obtained with low spinning rates (below 600 rpm) are those with better performances as energy converters. This fact is related both to the thickness of the films and to their morphology. We observed that the best-performing films contain both emissive and non-emissive grains
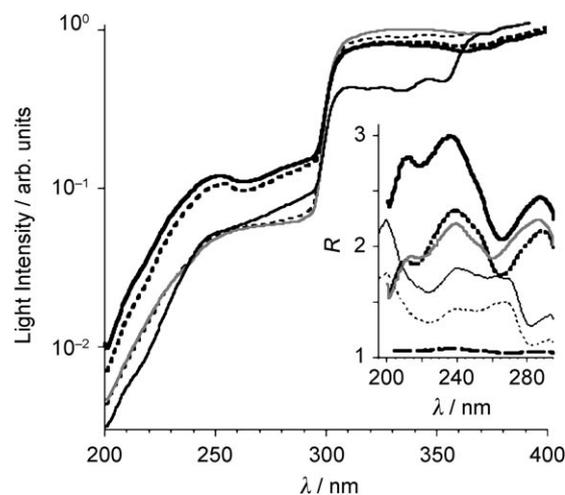
(see Figures 3 c, e). These films display balanced emission/diffusion properties in the transmission geometry, thus resulting in high emission efficiency without sensitive reduction of the light transmitted in the region of dye absorption. The films also show improved stability under UV illumination (see the Supporting Information).

Conclusions

We have prepared all-organic ICs based on PHTP and DCA hosts. Both host molecules crystallize and grow with the long axis oriented along the direction of the nanochannels, where emissive linear-chain molecules are inserted. Crystals of both types of ICs display host full-hole replenishment and emit polarized light. While PHTP-based ICs form inhomogeneous films, different film morphologies are obtained for the DCA ICs according to the preparation technique. Quite homogeneous thin films can be prepared by solution spin-coating. Dyes inserted in DCA show enhanced fluorescence properties, with quantum yields even higher than those of the solutions and emission colours that can be easily tunable from the blue to the white by co-inclusion of different dyes. We demonstrate that films of DCA ICs of DPB, DPH and P3, obtained by low-cost techniques such as solution casting and spin-coating, are able to convert NUV into visible light with an efficiency much higher than that of standard polymeric blends.

Experimental Section

Materials: DCA, T3, DPB and DPH were purchased from Sigma–Aldrich. T5 was synthesized as reported elsewhere.[15] All solvents were of analytical grade. PHTP was synthesized as reported in the literature.[7] PHTP ICs were obtained by co-evaporation of PHTP

and the dye molecules in high vacuum (10^{-6} mbar) onto cooled ($-30\,°C$) substrates, at rates of 0.3–1 Å min^{-1} for the dyes and about ten times higher for PHTP. Crystals of DCA ICs were obtained by slow evaporation of the host/guest mixture from different solvents (methanol,[12] methanol/acetonitrile, methanol/ethyl acetate, dimethyl sulfoxide) at room temperature under nitrogen flow with a host/guest ratio between 4:1 and 5:2. The DCA ICs were prepared from a DCA mother solution in methanol with a concentration of 0.01 mol L^{-1} and a guest mother solution (in the same mixture of solvents used for the DCA IC crystals) with a concentration of 0.005 mol L^{-1}. From the same mother solutions, co-ICs with P3 and DPH were prepared with P3/DPH ratios of 49.5:50.5 and 79.7:20.3, and a host/guest ratio of 2.5. DCA co-ICs with P3, DPH and T5 were prepared from a methyl ethyl ketone solution with P3/DPH/T5 ratios of about 98:1.4:0.6 and 50:48:2, and a host/guest ratio of 2.6. Films of DCA ICs were obtained by cast deposition or by spin-coating at spinning rates of 500 to 1500 rpm. The 1–5 wt % blends of DPB in PMMA were obtained from chloroform solution at a concentration of 25–30 g mL^{-1}. The DPB-PMMA film was obtained by spin-coating at 1500 rpm or by casting.

Structural and Morphological Characterization: A crystal selected from data collection (performed at ≈ 300 K), which showed well-defined faces and a yellowish colour and had approximate dimensions of $0.1 \times 0.2 \times 0.3$ mm^3, was examined using an Oxford Diffraction KM4 Xcalibur diffractometer fitted with a Sapphire 3 charge-coupled device (CCD) detector and using graphite-monochromated Mo$_{K\alpha}$ radiation. Data reduction (intensity integration and standard geometry and Lorentz-polarization correction) was performed with the CrysAlis software (Oxford Diffraction, 2007). The space group was identified as $P2_12_12_1$, and 11 872 reflections were measured of which 3354 were unique (average redundancy $= 3.5$); the R_{int} of redundant data was 0.046 and R_σ 0.060 (Friedel opposites merged). Reflections with $F_o > 4\sigma(F_o)$ were 1898 (see Supporting Information). Structure solution by means of direct methods and full-matrix least-squares refinement was performed with the crystallographic software SHELXS and SHELXL. Direct methods allowed determination of the DCA structure and individuation of three atoms of the DPH guest molecules (combined figure of merit $= 0.0649$). DCA molecules assume their configuration around a symmetry element (2_1 screw axis parallel to the c axis direction), hence forming the channel. Preliminary density maps were drawn with crystallographic software O and showed electron density along the channel axis, thus revealing the presence of three atoms, placed onto the 2_1 screw axis parallel to the a axis, which we presumed to belong to the six carbon atoms that form the centre of the DPH molecule. DCA H atoms were located geometrically and constrained to ride on their parent atoms with C–H(methine) $= 0.98$, C–H(methylene) $= 0.97$, C–H(methyl) $= 0.96$ Å and with U_{iso}(H) $= 1.2\,U_{eq}$(C). The disorder in the channel was modelled by means of a rigid model of DPH in *trans–trans* configuration, which was bound to DCA molecules and matched the positions of the three visible hexatriene carbon atoms. This rigid fragment was allowed to occupy the channel in two possible positions (shown later), whose occupancies were restrained to sum up to 0.25, to account for the two possible positions and site symmetry (2_1 parallel to a axis). The final occupancies for the A and B positions were one three times the other, namely 0.182(3) and 0.060(3). U_{iso} for atoms in DPH molecules was constrained to assume the same value for all atoms and converged to 0.097(2). The unit cell parameters yielded a volume of 2526.3(6) Å^3, that is, a density of 1.15 g cm^{-3}, fully consistent with other included DCA crystals (see Supporting Information).[17] AFM investigations were performed using an NT-MDT NTEGRA apparatus in tapping mode under ambient conditions.

Optical Characterization: PL continuous-wave measurements were obtained with an SPEX 270 M monochromator equipped with an N$_2$-cooled CCD and a monochromated Xe lamp. The spectra were corrected for the instrument response. The PL QY on solid-state materials was obtained by using a home-made integrating sphere[10, 30] and correcting the spectra of the low-emissive materials for the background of the exciting lamp, according to Equations (1) and (2):

$$QY = \frac{P_c^* - (1-A)P_b^*}{AL_a} \qquad (1)$$

$$P_{c/b}^* = P_{c/b} - \frac{L_{c/b}}{L_a}P_a \qquad (2)$$

where P and L are the integrated intensity of the PL spectra and the exciting lamp, respectively; index c refers to the measurement with the lamp impinging the sample, and b and a refer to the measurements with the lamp impinging the sphere with the sample inside and outside, respectively; $A = 1 - L_c/L_b$. Fluorescence microscopy images were collected with a Nikon Eclipse TE2000-U inverted confocal microscope with a long working distance using a Plan Apo VC objective (magnification 60× or 100×, NA 1.4). Excitation was obtained with a 100 W Hg lamp with a 330–380 nm band-pass excitation filter. For polarized measurements, a rotating polarizer was placed between the sample and the detectors. Ultrafast excitation experiments were performed by using subpicosecond pulses delivered either by an optical parametric amplifier (Light Conversion Topas), pumped by a Ti:sapphire amplified laser with 1 kHz repetition rate (Quantronix Integra, 1.5 mJ output energy), or by a frequency double-pulsed 80 MHz Ti:sapphire laser. Optical emission was spectrally dispersed in a single spectrometer and temporally resolved with a visible 2D-streak camera with a temporal resolution of 2 and 20 ps (Hamamatsu, C5680) for low and high repetition rates, respectively. Optical transmission measurements for the determination of energy conversion were performed with phase-sensitive modulation techniques by using a mechanically chopped 30-W monochromated deuterium lamp as light source, a custom Hamamatsu Si PIN photodiode with 9×9 mm^2 area detector and a Signal Recovery 7265 lock-in amplifier. The organic layer deposited onto a 10×10 mm^2 quartz plate was placed at a distance of 1 mm from the detector head.

Acknowledgements

[1] J. Cornil, D. A. Dos Santos, X. Crispin, R. Silbey, J. L. Brédas, *J. Am. Chem. Soc.* **1998**, *120*, 1289.

[2] D. F. Eaton, A. G. Anderson, W. Tam, Y. Wang, *J. Am. Chem. Soc.* **1987**, *109*, 1886.

[3] a) G. Bongiovanni, C. Botta, J. L. Brédas, J. Cornil, D. R. Ferro, A. Mura, A. Piaggi, R. Tubino, *Chem. Phys. Lett.* **1997**, *278*, 126; b) C. Botta, D. R. Ferro, G. Di Silvestro, R. Tubino in *Supramolecular Photosensitive and Electroactive Materials* (Ed.: H. S. Nalga), Academic Press, London, **2001**, chap. 5; c) G. Bongiovanni, C. Botta, G. Di Silvestro, A. Mura, R. Tubino, *Phys. Lett. A* **1995**, *208*, 165.

[4] a) G. Bongiovanni, C. Botta, G. Di Silvestro, M. A. Loi, A. Mura, R. Tubino, *Chem. Phys. Lett.* **2001**, *345*, 386; b) L. Poulsen, M. Jazdzyk, J.-E. Communal, J. C. Sancho-García, A. Mura, G. Bongiovanni, D. Beljonne, J. Cornil, M. Hanack, H.-J. Egelhaaf, J. Gierschner, *J. Am. Chem. Soc.* **2007**, *129*, 8585.

[5] J. Gierschner, L. Lüer, D. Oelkrug, B. Musluoglu, B. Behnisch, M. Hanack, *Adv. Mater.* **2000**, *12*, 757.

[6] M. Aloshyna, B. Milián Medina, L. Poulsen, J. Moreau, D. Beljonne, J. Cornil, G. Di Silvestro, M. Cerminara, F. Meinardi, R. Tubino, H. Detert, S. Schrader, H.-J. Egelhaaf, C. Botta, J. Gierschner, *Adv. Funct. Mater.* **2008**, *18*, 915.

[7] a) M. Farina, *Inclusion Compounds, Vol. 2* (Eds.: J. L. Atwood, J. E. D. Davis, D. D. MacNicol), Academic Press, London, **1984**, chap. 3; b) G. Allegra, M. Farina, A. Immirzi, A. Colombo, U. Rossi, R. Broggi, G. Natta, *J. Chem. Soc.* **1967**, 1020.

[8] O. König, H.-B. Bürgi, T. Armbruster, J. Hulliger, T. Weber, *J. Am. Chem. Soc.* **1997**, *119*, 10632.

[9] A. Quintel, F. Budde, P. Rechsteiner, K. Thoma, A. Zayats, J. Hulliger, *J. Mater. Chem.* **2000**, *10*, 27.

[10] C. Botta, S. Destri, M. Pasini, P. Picouet, G. Bongiovanni, A. Mura, M. Uslenghi, G. Di Silvestro, R. Tubino, *Synth. Met.* **2003**, *139*, 791.

[11] a) H. Sobotka, *Chem. Rev.* **1934**, *15*, 311; b) H. Wieland, H. Sorge, *Hoppe-Seyler's Z. Physiol. Chem.* **1916**, *97*, 1.

[12] a) A. Jover, F. Meijide, V. H. Soto, J. Vazquez Tato, E. Rodriguez Nunez, H. T. Ton-Nu, A. F. Hofmann, *Steroids* **2004**, *69*, 379; b) K. Kato, M. Sugahara, N. Tohnai, K. Sada, M. Miyata, *Eur. J. Org. Chem.* **2004**, 981.

[13] M. Szyrszyng, E. Nowak, M. Gdaniec, M. J. Milewska, T. Polonski, *Tetrahedron: Asymmetry* **2004**, *15*, 3257.

[14] Z. S. Wang, Y. Cui, Y. Dan-oh, C. Kasada, A. Shinpo, K. Hara, *J. Phys. Chem. C* **2007**, *111*, 7224.

[15] C. Botta, G. Patrinoiu, P. Picouet, S. Yunus, J. E. Communal, F. Cordella, F. Quochi, A. Mura, G. Bongiovanni, M. Pasini, S. Destri, G. Di Silvestro, *Adv. Mater.* **2004**, *16*, 1716.

[16] C. P. Tang, H. C. Chang, R. Popovitz-Biro, F. Frolow, M. Lahav, L. Leiserowitz, R. K. McMullan, *J. Am. Chem. Soc.* **1985**, *107*, 4058.

[17] K. Takazawa, Y. Kitahama, Y. Kimura, G. Kido, *Nano Lett.* **2005**, *5*, 1293.

[18] R. Bosisio, C. Botta, A. Colombo, S. Destri, W. Porzio, E. Grilli, R. Tubino, G. Bongiovanni, A. Mura, G. Di Silvestro, *Synth. Met.* **1997**, *87*, 23.

[19] MATSTUDIO modelling release 4.1, Accelrys Inc., 9685 Scranton Rd., San Diego, CA (USA) **2006**. (www.accelrys.com).

[20] C. E. Bunker, C. A. Lytle, W. Rollins, Y.-P. Sun, *J. Phys. Chem. A* **1997**, *101*, 3214.

[21] J. Saltiel, T. S. R. Krishna, R. J. Clark, *J. Phys. Chem. A* **2006**, *110*, 1694.

[22] DCA ICs of DPH obtained from the rapidly evaporating CH$_2$Cl$_2$ solvent show spectral shapes similar to the solution spectra, where a *cis* component is present.

[23] B. E. Kohler, T. Itoh, *J. Phys. Chem.* **1988**, *92*, 5120.

[24] J. Saltiel, D. F. Sears, Jr., Y.-P. Sun, J.-O. Choi, *J. Am. Chem. Soc.* **1992**, *114*, 3607.

[25] A. M. Turek, G. Krishnamoorthy, D. F. Sears, Jr., I. Garcia, O. Dmitrenko, J. Saltiel, *J. Phys. Chem. A* **2005**, *109*, 293.

[26] S. K. Chattopadhyay, P. K. Das, G. L. Hug, *J. Am. Chem. Soc.* **1982**, *104*, 4507.

[27] E. D. Cehelnik, R. B. Cundall, J. R. Lockwood, T. F. Palmer, *J. Phys. Chem.* **1975**, *79*, 1369.

[28] Y. Sonoda, Y. Kawanishi, T. Ikeda, M. Goto, S. Hayashi, Y. Yoshida, N. Tanigaki, K. Yase, *J. Phys. Chem. B* **2003**, *107*, 3376.

[29] D. Paneque, H. J. Gebauer, E. Lorenz, M. Martinez, K. Mase, R. Mirzoyan, A. Ostankov, T. Schweizer, *Nucl. Instrum. Methods Phys. Res. Sect. A* **2003**, *504*, 109.

[30] J. C. de Mello, H. F. Wittmann, R. H. Friend, *Adv. Mater.* **1997**, *9*, 230.